Chapter 19
Substructure Pseudo-Dynamic Tests on Seismic Response Control of Soft-First-Story Buildings

Hideto Kanno, Tetsuya Nishida, and Jun Kobayashi

Abstract Soft-first-story structures, such as piloti buildings, are known as vulnerable structures against earthquakes. In this chapter, a simple scheme for reducing the structural damage of such buildings is proposed. Its effectiveness is experimentally examined through substructure pseudo-dynamic tests. In the proposed method, low yield strength steel devices are applied as elasto-plastic dampers at the first story of the buildings to reduce the seismic response and damage. A six-story single-span piloti model, with or without steel dampers, are the subject of the test. The behavior of the two exterior columns at the first story and the steel damper are tested. The substructure pseudo-dynamic tests are successfully performed to investigate the elasto-plastic behavior of the damper and the reinforced concrete columns at the soft-first-story, as well as the overall structural performance. The experimental results show that the seismic damage of piloti buildings can be reduced with steel dampers, which have been found to work as effectively as expected.

19.1 Introduction

Soft-first-story structures, such as piloti buildings, are vulnerable against earthquake (Naeim and Lew 2000). In the 1995 Kobe earthquake, some piloti buildings designed with modern design codes, as well as many older buildings, suffered serious structural damage. Most of the damage was concentrated at the first story, owing to the change in lateral stiffness and strength compared to the upper part of the structure. One way to reduce the seismic damage of such structures is to increase the column section at the first story, in order to reduce the stiffness discontinuity (Kaushik et al. 2009 and Lu et al. 1999). However, this causes construction

H. Kanno (✉) • T. Nishida • J. Kobayashi
Department of Architecture and Environment Systems, Faculty of Systems Science and Technology, Akita Prefectural University, 84-4 Ebinokuchi, Tsuchiya, Yurihonjo, Akita 015-0055, Japan
e-mail: kanno@akita-pu.ac.jp; tetsuya_nishida@akita-pu.ac.jp; jun_kobayashi@akita-pu.ac.jp

A. Ilki and M.N. Fardis (eds.), *Seismic Evaluation and Rehabilitation of Structures*, Geotechnical, Geological and Earthquake Engineering 26,
DOI 10.1007/978-3-319-00458-7_19,

problems, due to the discontinuity of the main bars of the columns. Another way is to dissipate seismic energy in the soft-first-story using dynamic dampers, thus taking advantage of the concentration of structural deformations in the soft story (Iqbal 2006, Mezzi and Parducci 2005 and Todorovska 2008). In this chapter a simple scheme is proposed in order to reduce structural damage in such piloti buildings, using low-yield-strength-steel devices as elasto-plastic dampers in the first story. The detailed response of such buildings depends on the precise elasto-plastic behavior of the steel dampers. The shape of the hysteresis loop of the steel damper, including fatigue behavior, is particularly important. A full size test seems to be almost impossible; therefore a scaled model and the substructure pseudo-dynamic test method were conceived for this purpose.

In this study, six-story piloti reinforced concrete (RC) frames are experimentally tested, in order to examine the effectiveness of steel dampers in reducing the structural damage. Two sets of structural models are compared to each other through substructure pseudo-dynamic tests.

19.2 Outline of the Tests

19.2.1 Building Model

Figure 19.1 shows the prototype of the six-story single-span piloti frame. Its transverse span is 9 m. The height of the first story is 3.5 m and that of the upper floors is 3.1 m. There are four spans in the longitudinal direction of the building. The central single frame in the transverse direction is considered under one-directional in-plane loading. The steel damper is placed between the lower and the upper beam at the first story of the frame. The connections of the damper are assumed to be rigid, and their deformations are neglected.

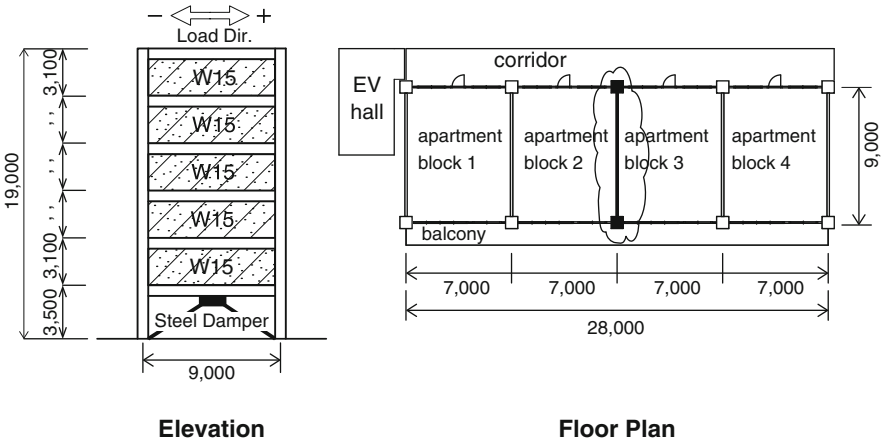

Fig. 19.1 Model frames (*dimensions in mm*)

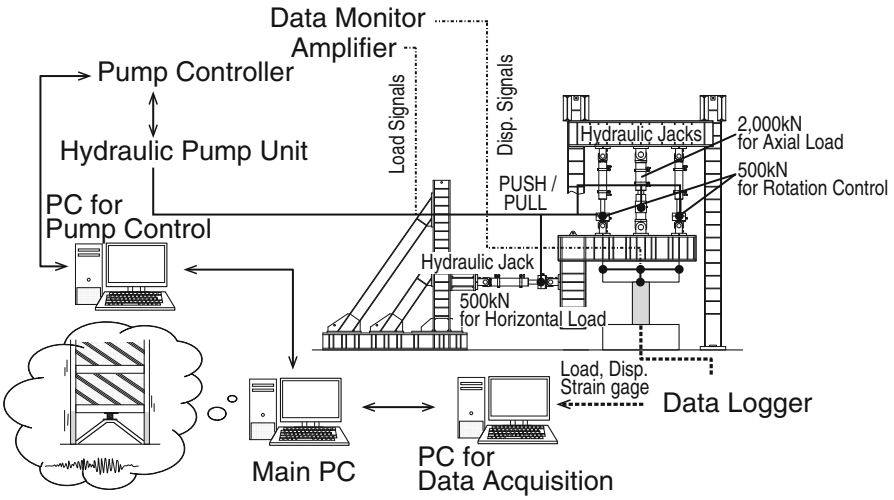

Fig. 19.2 Schematic diagram of testing system

19.2.2 Testing System

In order to conduct the substructure pseudo-dynamic test, the prototype structure is modelled in two parts. One is the actual specimen which is experimentally tested so that the elasto-plastic behavior of the critical part of the structure is realistically represented. The behavior of the other part, which is expected not to critically affect the total response of the structure, is numerically calculated using a conventional nonlinear computational approach. The substructure pseudo-dynamic test is developed on a basis of pseudo-dynamic testing, which is an experimental technique for simulating the seismic response of the tested structure or component.

In the present tests, two exterior columns and a steel damper on the first floor are the tested part, which are represented by three separate specimens. Figure 19.2 shows the scheme of pseudo-dynamic testing developed at the Akita Prefectural University (Teramoto et al. 2008). The system consists of the main management part (Main PC), the data acquisition and the hydraulic pump control. The main management part controls the system and executes the numerical analysis during the tests. The main PC sends command signals, such as the target displacement for each tested part, to the hydraulic pump control unit, so that the target displacement can be reached. Then the measured information, such as the restoring forces and moments of the tested parts, is sent back to the Main PC together with analytical results of the numerical models to calculate the total structural behavior. The loading conditions for the tested part, the deformations, axial loads and rotation angles of beam-column connections, are calculated step by step prior to the next step of the loading. Loading is carried out with an accuracy of 0.01 mm using servo-controlled hydraulic jacks. Loads in the two directions, horizontal and vertical, and the moment at the column top, are measured simultaneously.

The integration method using the operator-splitting (OS) method was applied in the tests. This method has been used in many Substructure pseudo-dynamic experiments to calculate the seismic response considering the interaction between the specimen and the whole frame (Nakashima et al. 1990). The formulation of this method is as follows:

$$Ma_{n+1} + Cv_{n+1} + K^I d_{n+1} + K^E_{n+1} d_{n+1} = P_{n+1} \tag{19.1}$$

$$\tilde{d}_{n+1} = d_n + v_n \Delta t + a_n \left(\frac{\Delta t}{2}\right)^2 \tag{19.2}$$

$$d_{n+1} = \tilde{d}_{n+1} + a_{n+1} \left(\frac{\Delta t}{2}\right)^2 \tag{19.3}$$

$$v_{n+1} = v_n + (a_n + a_{n+1}) \left(\frac{\Delta t}{2}\right) \tag{19.4}$$

In Eqs. (19.1), (19.2), (19.3) and (19.4) K^I and K^E_{n+1} are the linear and the non-linear stiffness matrices, M and C are the mass and viscous damping matrices, $\tilde{d}$ and d are the predictor and corrector displacement vectors, v and a are the velocity and acceleration vectors, and Δt is the integration time interval, respectively. The main characteristic of this method is the division of the stiffness of the whole structure into a linear and a non-linear stiffness. For the non-linear tested part, the explicit predictor-corrector method is used.

The Newmark's β method (linear stiffness integration method) is also applied to take account of the non-linear part of the whole structure. If the linear stiffness is much larger than the non-linear stiffness, the integration method is unconditionally stable. In this work, the equations were transformed into an incremental form. It was confirmed that even when the incremental form of the equations is applied, the condition where the linear stiffness is larger than the non-linear tangent stiffness ensures that the integration method gives a stable solution.

The procedure for the substructure pseudo-dynamic tests in this study is as follows:

1. By using the integration method (OS method), the target predictor displacement at the next step is calculated. The Main PC (shown in Fig. 19.2) is used in this calculation.
2. The main PC sends the target displacement (horizontal displacement and rotation angle at the top of the column and steel damper) to the PCs for the Pump Control Unit of each specimen (the two RC columns and the steel damper).

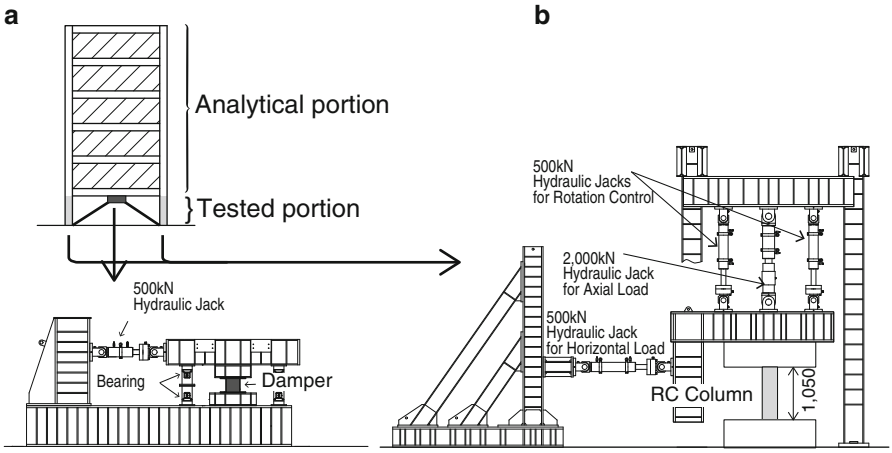

Fig. 19.3 Set up for tested parts. (**a**) Test setup for the damper. (**b**) Test setup for RC columns

3. Until the current displacement reaches the target value, the specimens are loaded by the four jacks (one jack in the case of the damper) under the control.
4. The restoring forces (horizontal load and moment at the top of the column) are measured when the displacements reach the target value by the load cells attached to the jacks, and the values are fed back to the Main PC.
5. After the restoring forces are fed back to the Main PC, the latter sends a command to the PC for Data Acquisition.
6. After the data acquisition is completed, step 1 is carried out using the data on the restoring force and the input acceleration.

19.2.3 Tested Part

The test setups are shown in Fig. 19.3. In this study, two RC specimens and one steel damper on the first floor are tested individually but concurrently. Therefore two kinds of loading systems are provided. Each specimen must be loaded simultaneously with the analytical calculated loads coming from the upper part of the framed structure. Therefore, four static hydraulic actuators are connected to each column specimen, so that loading with three degree of freedom can be performed. One actuator is connected to the damper and loading takes place with one degree of freedom. In the case of RC column, as shown in Fig. 19.3b, the middle actuator in the vertical direction has a loading capacity of 2,000 kN; the force capacity of the other two vertical actuators and one horizontal actuator is 500 kN. The force capacity of the horizontal actuator for the damper is 500 kN.

The specimens for the RC columns are shown in Fig. 19.4. The size of the column is 300 $\times$ 300 mm and its clear height 1.05 m, at a 3:8 scale of the prototype

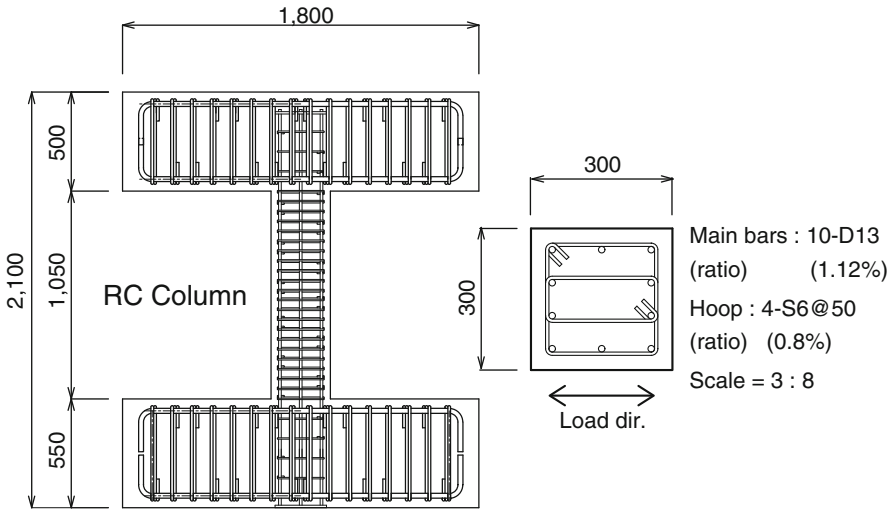

Fig. 19.4 Details of the RC column

building. The main reinforcement consists of ribbed (deformed) 13 mm bars with an average yield strength of 377 N/mm^2. The shear reinforcement consists of ribbed (deformed) 6 mm high strength bars, with an average strength of 1,100 N/mm^2. The compressive strength of the concrete is 38.8 N/mm^2.

The steel damper is designed so that about 10 % of the critical damping can be provided to the building model. Figure 19.5 shows details of the low-yield-strength steel damper.

The steel damper is panel-shaped, with dimensions of 262 mm by 262 mm and 6 mm thickness. A full-scale model is used for the damper, to provide realistic elasto-plastic hysteretic behavior. The low yield strength steel has an average yield strength of 154 N/mm^2.

19.2.4 Analytical Models

In the analytical part, shear walls in the upper part of the building are modeled as elastic axial springs and elasto-plastic shear springs. Multi-springs (MS) are added to both end sections of shear walls, as illustrated in Fig. 19.6. The MS model consists of five layers of steel and concrete springs at selected locations. These springs are assumed as individual axial springs, representing the stiffness of the longitudinal reinforcement and the concrete. A shear spring is used to represent the shear hysteretic behavior of the shear wall. In this study, the beams connecting to shear walls are treated as rigid at both ends of the shear wall.

The hysteretic characteristics of the reinforcement and the concrete are shown in Fig. 19.7. The force-deformation relationship with a bilinear skeleton curve for

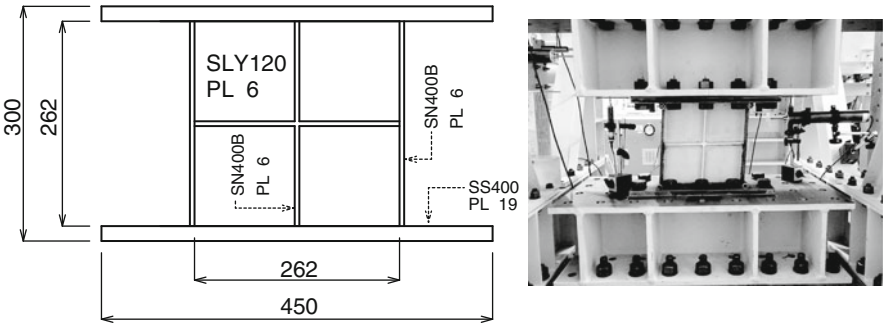

Fig. 19.5 Details of the low-yield-strength steel damper

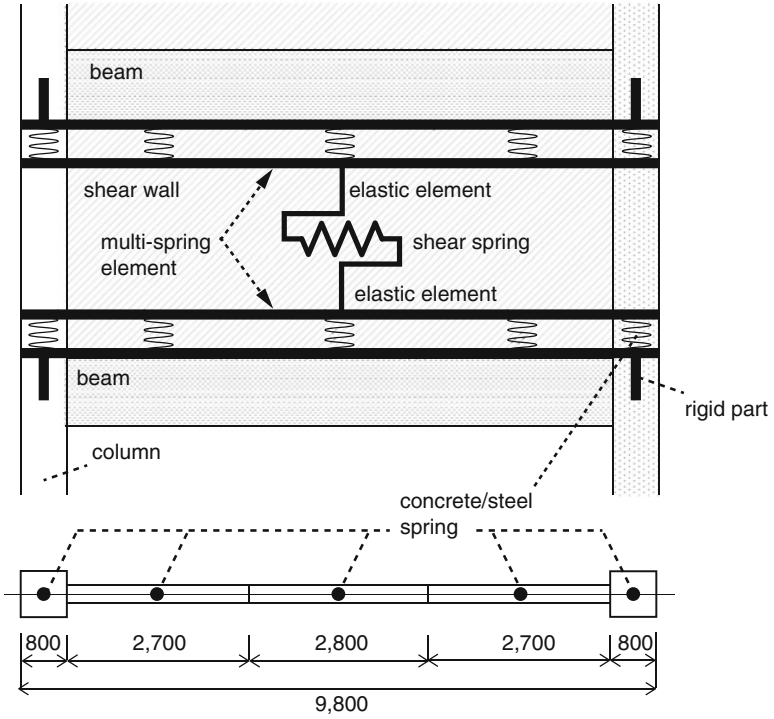

Fig. 19.6 Analytical model for shear walls

steel springs (the reinforcement) is shown in Fig. 19.7a, where f_s and d_s are axial force and deformation of the steel spring, respectively, and f_{sy}, d_y are the yield strength and yielding deformation. The unloading stiffness is assumed equal to the initial stiffness of the steel spring.

The hysteretic relationship for the concrete spring is assumed for simplicity as a tri-linear skeleton curve, as shown in Fig. 19.7b, where f_c and d_c are axial force and axial deformation of the concrete spring respectively; f_{cy} is the compressive

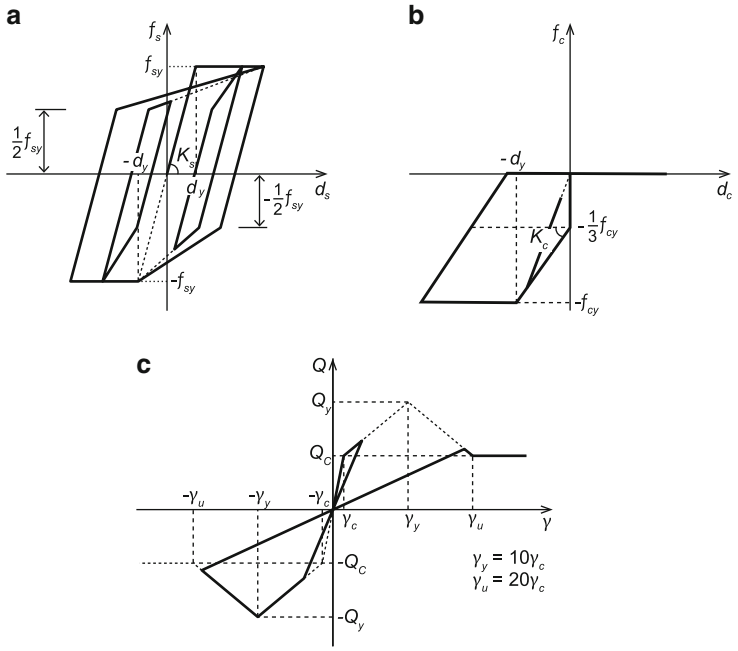

Fig. 19.7 Hysteretic model for axial (steel and concrete) and shear springs. (**a**) Steel spring. (**b**) Concrete spring. (**c**) Shear spring

strength of the concrete spring. The tensile resistance of concrete is neglected. The post-peak degradation of the concrete spring is not considered. The initial stiffness of the concrete spring is taken as infinitely rigid. The stiffness degrading behavior after the initial stiffness level is taken into account, when the axial stress is larger than $f_{cy}/3$.

Regarding the shear springs, it is assumed that shear has no effects on the axial force and bending interaction. The hysteretic model for the shear spring is assumed to be multi-linear model, as shown in Fig. 19.7c, where Q is shear force and γ the deflection of the shear wall due to shear deformation. The value of the shear force and deflection at cracking and yielding can be calculated according to the formulations proposed by the Architectural Institute of Japan.

Two series of substructure pseudo-dynamic tests were conducted. One on a piloti frame with the steel damper placed in the soft first story; the other on the piloti frame only without the steel damper, to confirm the damper effect. In these tests, the integration time interval was 0.01 s. Rayleigh damping was applied and the viscous damping ratio was set at 3 %. A simulated earthquake ground motion as shown in Fig. 19.8 was used, based on the phase characteristics of the El Centro 1940 record. The target spectral characteristic was based on the design spectrum specified in the Japanese building design code. Both series of tests, with the damper or without, were divided in three stages, from weak elastic response (RUN1) to the strong inelastic level (RUN3). After RUN3 (the maximum test level), the second stage level was carried out again as RUN4 to study the aftershock response.

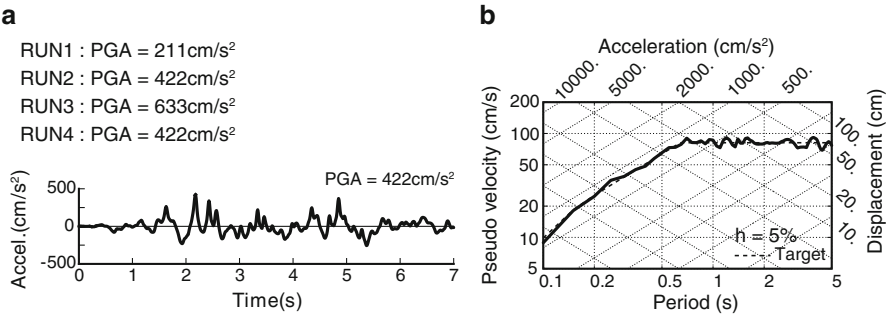

Fig. 19.8 Input motion. (**a**) Input wave. (**b**) Response spectrum

19.3 Results of Tests

19.3.1 Outline of Test Results

Figure 19.9 shows base shear-story drift hysteresis loops obtained from the tests. Figure 19.10 depicts the shear force-deformation relationships of the tested members during RUN3. The upper part of each figure refers to the piloti frame without a damper and the bottom one to the case with the damper. It can be seen that when the damper is used in the soft-first-story the performance of the piloti frame is good, especially at larger excitation levels.

During RUN1 both models (with or without a damper) show almost elastic behavior. In the model without a damper, some main bars yielded at the bottom of the RC column during RUN2. In the subsequent loading RUN3 all reinforcing bars yielded and the story drift angle reached about 12.5 mrad. By contrast, in the model with the damper, only some of the main bars yield during RUN3 and the peak displacement does not exceed half of that of the model without damper. During RUN4, which represents the behavior in an aftershock, both models show larger response than RUN2; however, the model with a damper has much lower displacement response than the one without a damper.

The peak lateral load distributions in both tests are shown in Fig. 19.11. Some studies (e.g. Lu et al. 1999) suggest that, in piloti structures the maximum lateral load on each floor is uniformly distributed, because most of the displacement tends to concentrate in the first story. The results of the present research confirm those findings, even when there is a damper at the soft-first-story.

19.3.2 Energy Response

The seismic energy response of soft-first-story frames is discussed based on the results of the substructure pseudo-dynamic tests. The total input energy, E_I, and

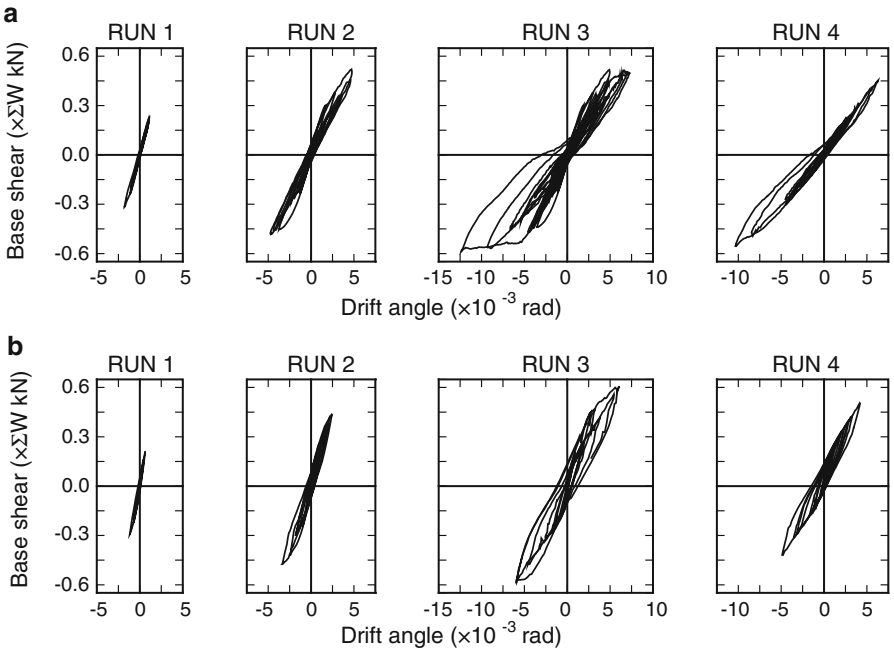

Fig. 19.9 Base shear-drift angle relationships (test results). (**a**) w/o damper. (**b**) With damper

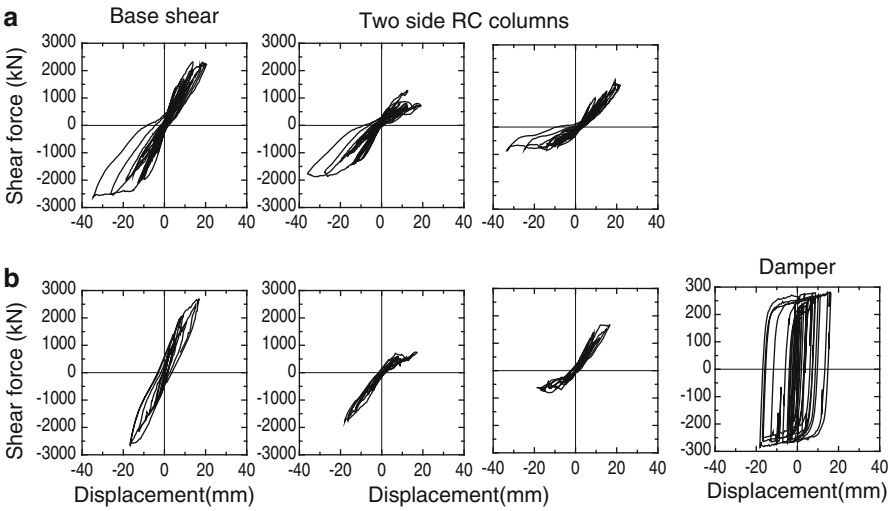

Fig. 19.10 Shear force-deformation relationships of tested members during RUN3. (**a**) w/o damper. (**b**) With damper

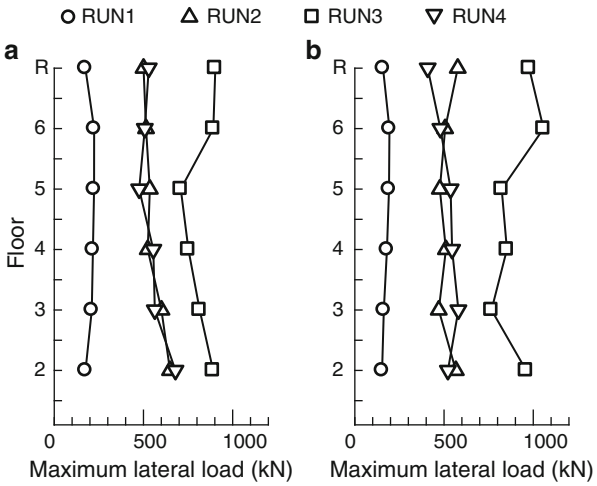

Fig. 19.11 Maximum lateral load distributions in both tests. (**a**) w/o damper. (**b**) With damper

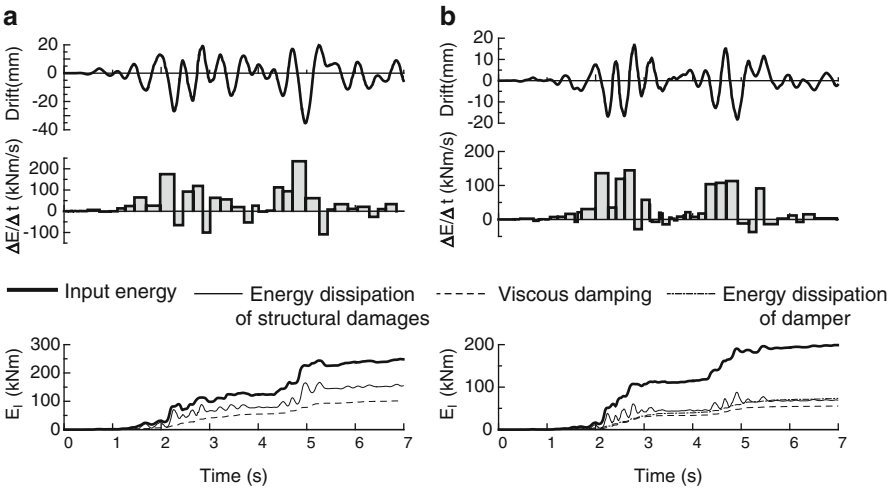

Fig. 19.12 Time history of energy response during RUN3. (**a**) w/o damper. (**b**) With damper

the momentary input energy, ΔE, are discussed dividing the input energy into hysteretic energy dissipation in the RC columns (in the lateral and the axial direction) of the soft-first-story and in the shear walls of the upper story, viscous damping and energy dissipation in the dampers of the first story. By momentary input energy is meant the increment of seismic input energy in half a cycle of the response (Nakamura et al. 1998). Figure 19.12 shows the time-histories of displacement and seismic response energy, ΔE and E_I, during RUN3, which is the maximum level of loading in the tests. It can be seen that, in both tests, ΔE is large when the displacement is increased. Figure 19.13 shows the relationships between the

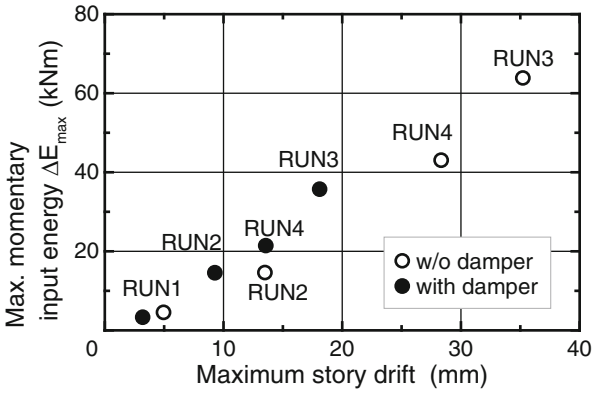

Fig. 19.13 Maximum moment input energy-maximum story drift relationships

maximum momentary input energy $\Delta E_{\max}$ and the maximum drift of the first story. It suggests that $\Delta E_{\max}$ reflects the intensity of the energy input, related to the peak response displacement during the transient response.

Figure 19.14 shows the ratio of dissipated energy to seismic input in each stage of testing. In the cases without a damper, the energy dissipated by the RC columns is about 40–50 % of the input energy; the viscous damping energy is about 30–40 %. This tendency is observed in all the stages and input levels. When using the damper, the energy dissipation by the damper is very large (about 40 % of the total energy). As a result, the energy dissipation due to column damage and viscous damping is less than the one without the damper. More specifically, the energy dissipation ratio during RUN4 shows that the steel damper worked adequately, even for comparatively large aftershocks.

19.4 Conclusion

Substructure pseudo-dynamic tests were successfully performed to investigate the dynamic behavior of the reinforced concrete columns of the soft-first-story and of the damper placed in that story, as well as the total structural performance. Experimental results indicate that the seismic damage of piloti buildings can be reduced with steel dampers, as these worked as effectively as expected. More specifically, the steel dampers provide good performance during the largest ground motion and large aftershocks. The maximum response displacement has a stronger correlation with the maximum momentary input energy, $\Delta E_{\max}$, than with the amount of total input energy, because of the characteristics of the inelastic behavior of RC structures during earthquakes.

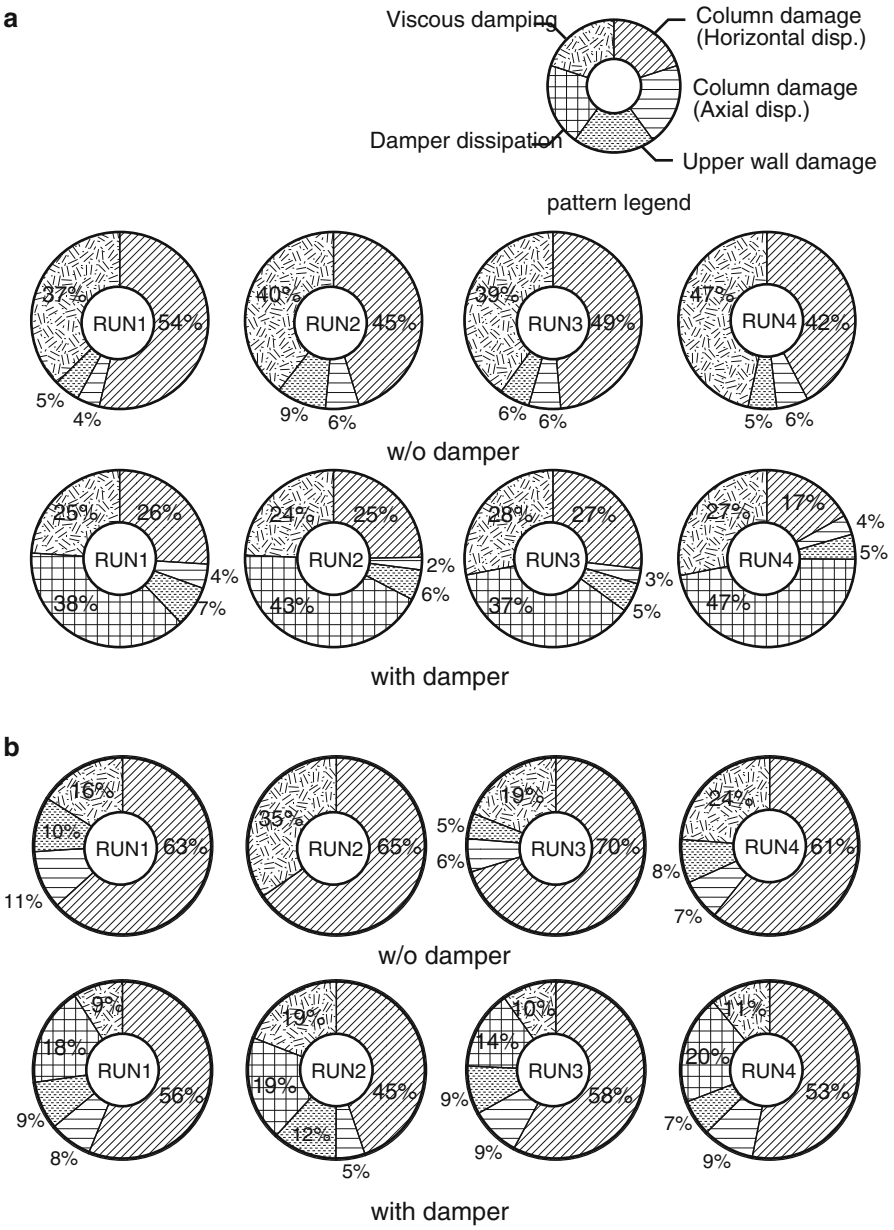

Fig. 19.14 Energy dissipation ratio. (**a**) Total input energy. (**b**) Maximum momentary input energy

References

Iqbal A (2006) Soft first storey with seismic isolation system. In: NZSEE conference, Napier, CDROM paperID 36

Kaushik HB, Rai DC, Jain SK (2009) Effectiveness of some strengthening options for masonry-infilled RC frames with open first storey. J Struct Eng ASCE 135(8):925–937

Lu Y, Tassios TP, Zhang G-F, Vintzileou E (1999) Seismic response of reinforced concrete frames with strength and stiffness irregularities. ACI Struct J 96(2):221–229

Mezzi M, Parducci A (2005) Preservation of existing soft-first-storey configurations by improving the seismic performance. In: 3rd specialty conference on the conceptual approach to structural design

Naeim F, Lew M (2000) The 1999 earthquake disasters worldwide: how many times do we have to re-learn the fundamentals of seismic engineering? Struct Des Tall Build 9(2):161–182

Nakamura T, Hori N, Inoue N (1998) Evaluation of damaging properties of ground motions and estimation of maximum displacement based on momentary input energy. J Struct Constr Eng (in Japanese) 513:65–72

Nakashima M, Kaminosono T, Ishida M, Ando K (1990) Integration techniques for substructure pseudo-dynamic test. In: 4th US national conference on earthquake engineering, vol 2, pp 512–524

Teramoto N, Nishida T, Kobayashi J (2008) Structural performance of side columns subjected to varying axial load. In: 14th world conference on earthquake engineering, paper-ID 05-03-0234

Todorovska MI (1999) Base isolation by a soft first storey with inclined columns. J Eng Mech ASCE 1254:448–457